Lithuanian Journal of Physics, Vol. **47**, No. 1, pp. 63–68 (2007) doi:10.3952/lithjphys.47110

SOL–GEL PREPARATION OF NANOCRYSTALLINE $CaWO_4$

A. Katelnikovas [a], L. Grigorjeva [b], D. Millers [b], V. Pankratov [b], and A. Kareiva [a]

[a] *Faculty of Chemistry, Vilnius University, Naugarduko 24, LT-03225 Vilnius, Lithuania*
[b] *Institute of Solid State Physics, University of Latvia, Kengaraga 8, LV-1063 Riga, Latvia*
E-mail: aivaras.kareiva@chf.vu.lt

Received 1 December 2006

Nanocrystalline $CaWO_4$ has been synthesized by a sol–gel method using tungsten (VI) oxide, WO_3, and calcium nitrate tetrahydrate, $Ca(NO_3)_2 \cdot 4H_2O$ as starting materials. The synthesis leads to a sol–gel process when citric or tartaric acids are introduced into the solution obtained by dissolving WO_3 in ammonia. Citric and tartaric acids have great effect on stabilizing the precursor solution. The results have shown that the single phase product was obtained when the gel was heat-treated at 800 °C. The obtained $CaWO_4$ particles ranged from 350 to 850 nm in size and showed emission in the blue region. $CaWO_4$ ceramics has been characterized by means of thermogravimetric and differential thermal analysis (TG / DTA), infrared spectroscopy (IR), X-ray diffraction (XRD), scanning electron microscopy (SEM), and photoluminescence (PL).

Keywords: calcium tungstate, sol–gel, X-ray diffraction, photoluminescence

PACS: 42.70.-a, 61.46.-w, 68.37.Hk, 78.67.Bf

1. Introduction

Different multinary metal oxide ceramics are promising materials for optical and electronic applications [1, 2]. These compounds doped with transition metals or lanthanide elements are important materials which could be widely used in luminescence systems, window materials for a variety of light sources, and for fibre-optic telecommunication systems. These oxides are also widely applied as phosphors in cathode-ray tubes (projection TV sets), field emission, vacuum fluorescent, and electroluminescent displays as well as scintillators in X-ray and positron emission tomographs [1–3]. The specific luminescence properties of metal oxide ceramics are highly sensitive to the host material, dopant composition and concentration, host stoichiometry, and processing conditions.

Rare earth ion-doped tungstate crystals prepared by different methods have received much attention as promising laser materials, especially due to their attractive third-order nonlinear dielectric susceptibilities [4–6]. Because of their attractive luminescence and structural properties, tungstates have been intensively studied and applied in many fields such as lasers, fluorescent lamps, and scintillators during the last few decades. Tungstates can be divided into two groups with different crystal structure: scheelites ($CaWO_4$, $BaWO_4$, $SrWO_4$, and $PbWO_4$) and wolframites ($MgWO_4$, $CdWO_4$, $ZnWO_4$, and others) [7]. As a representative example, calcium tungstate $CaWO_4$ with the scheelite structure, containing Ca^{2+} ions and $WO_4{}^{2-}$ groups with the coordination number of eight for Ca^{2+} and four for W^{6+}, is considered to be a highly functional material due to its intriguing luminescent properties. It mainly shows efficient blue emission excited by short-wavelength ultraviolet radiation, X-rays, cathode rays, etc. Thus, $CaWO_4$ is an important optical material, which has attracted particular interest because of its practical applications such as laser host materials in quantum electronics and scintillators in medical devices [8]. Moreover, $CaWO_4$ has shown considerable promise as fibre–matrix interlayer in all-oxide ceramic composites [9].

Owing to such wide and diverse application potential of $CaWO_4$ ceramics, new routes for the synthesis of pure and homogeneously doped calcium tungstate are highly desirable. In the recent years intense effort has been witnessed in preparation of nanomaterials thanks to their markedly different physical and chemical properties as compared to bulk materials [10–11]. To date, most efforts of calcium tungstate preparation have been directed to single crystals, powders, and films of $CaWO_4$. However, the reports on the preparation of nano-sized $CaWO_4$ are very rare. Such situation has initiated the present work, motivating us to continue

ISSN 1648-8504

the investigations towards the development of synthesis routes for the preparation of nano-sized $CaWO_4$. The sinterability and physical properties of $CaWO_4$ synthesized by an aqueous sol–gel process were investigated in the present study.

2. Experimental procedure

For the sol–gel preparation of $CaWO_4$ the following analytical grade reagents were used: tungsten oxide (WO_3, Merck); calcium nitrate tetrahydrate ($Ca(NO_3)_2{\cdot}4H_2O$, Aldrich); nitric acid (HNO_3, Lachema); ammonia ($NH_3{\cdot}4H_2O$, Lachema); tartaric acid ($C_4H_6O_6$, Aldrich); citric acid ($C_6H_8O_7$, Aldrich).

The $CaWO_4$ samples were prepared by aqueous nitrate-tartrate (TAS) and nitrate-citrate (CAS) sol–gel routes. Stoichiometric amounts of analytical grade WO_3 and $Ca(NO_3)_2{\cdot}4H_2O$ were used as starting materials. In the sol–gel process WO_3 was first dissolved in 30 ml of concentrated ammonia solution by stirring at 70 °C. The excess of ammonia was neutralized by concentrated HNO_3 until pH reached the value of $\sim$6.0. Secondly, tartaric acid (TA) or citric acid (CA) with a molar ratio of $W/TA(CA) = 0.25$ dissolved in a small amount of distilled water was added with continuous stirring during several hours at the same temperature. Next, the stoichiometric amount of calcium nitrate dissolved in distilled water was mixed with previous solution. Finally, the same amount of an aqueous solution of the complexing agent was repeatedly added to the reaction mixture preventing crystallization of metal salts during gelation. The beaker with solution was closed with a watch glass and left with continuous stirring for 10–15 min. The obtained solution was concentrated by slow evaporation (8 h) at 70 °C in an open beaker. When nearly 90% of water was evaporated under continuous stirring, the brownish transparent gels formed. After drying in an oven at 105 °C, a fine-grained powder was obtained. The precursor powders were calcined for 5 h at 500 °C in alumina crucibles and reground carefully in an agate mortar. Since the gels are very combustible, slow heating (1 °C/min), especially between 150 and 350 °C, was found to be essential. After the intermediate grinding step the powders were annealed for 1 h at 800 °C in air at ambient pressure.

The thermal analysis (TG / DTA) measurements were performed with a STA 490 analyzer (Netzsch) in the air atmosphere at a heating rate of 10 °C/min. The synthesized samples were characterized by X-ray powder analysis (STOE Powder Diffraction System) using Cu $K_{\alpha 1}$ radiation, spectra were recorded at the standard rate of 1.5 2Θ/min. After pressing the samples into pellets with KBr ($\sim$1.5%), the infrared (IR) spectra were recorded with a Perkin–Elmer FT-IR Spectrum 1000 spectrometer. The scanning electron microscope (SEM) DSM 962 was used to study the surface morphology and microstructure of the ceramic samples. The luminescence properties of $CaWO_4$ samples were studied at room temperature on the Edinburgh Instruments based spectrometer system. Its light source was a deuterium lamp, a vacuum monochromator (Acton Research), and a refocusing unit evacuated by a directly flanged turbo drag pump. The samples were kept under a constant flow of dry nitrogen. Detection of the emitted light was done via a collecting optics, a monochromator, and a photomultiplier tube (Hamamatsu).

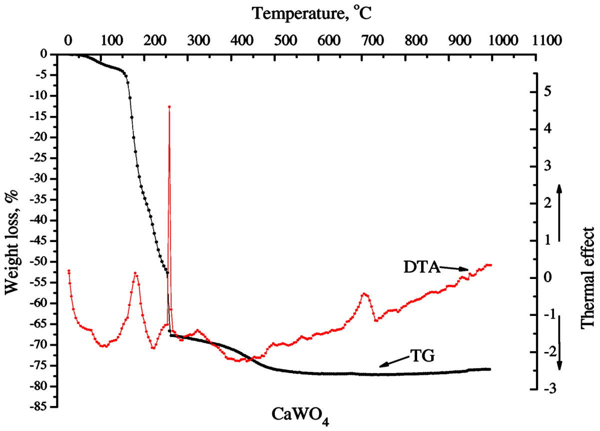

Fig. 1. TG / DTA curves for the Ca-W-O nitrate-tartrate gel.

3. Results and discussion

The mechanism of thermal decomposition of the dried Ca-W-O nitrate-tartrate and nitrate-citrate gels in the flowing air was studied by TG / DTA measurements. TG / DTA curves showed that in both cases the thermal decomposition proceeded in a similar way. The representative TG / DTA curves for the precursor gel obtained by the nitrate-tartrate (TAS) sol–gel route are shown in Fig. 1. It can be seen that the TG curve shows three main weight losses in the temperature range of $\sim$20–550 °C. The decomposition started below 150 °C ($\sim$5%) with a loss of crystallization water and / or water from the coordination sphere of the metal complexes. Further increasing the temperature from 150 to 250 °C, the pyrolysis of the gel occurs, as has been indicated by sharp weight loss ($\sim$60%) on the TG curve. The last continuous weight loss ($\sim$10%) observed in the temperature range of $\sim$250–550 °C is associated with fur-

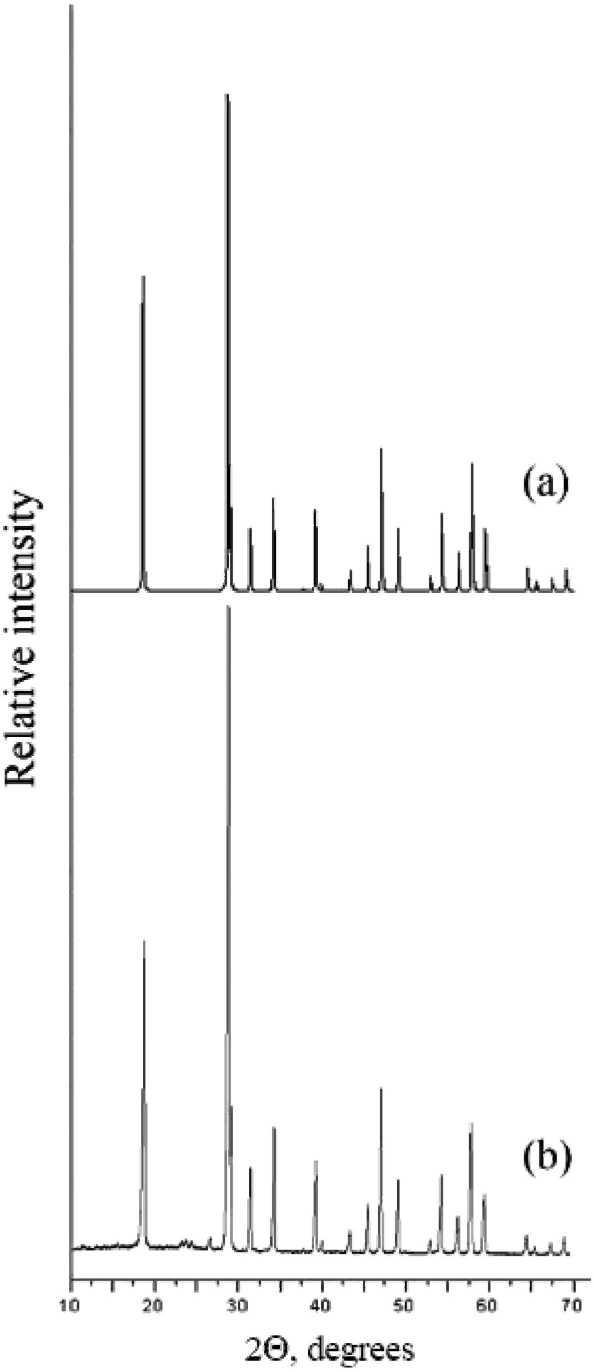

Fig. 2. Powder XRD patterns of $CaWO_4$ samples obtained by different sol–gel synthesis routes: (a) TAS and (b) CAS.

ther decomposition of the gel and intermediate pyrolysis products (i. e., $CaCO_3$).

The thermal decomposition behaviour is associated with endothermic and exothermic effects in the DTA curve. The broad and weak endothermic peak in the low temperature region (∼80–100 °C) on the DTA curve indicates that dehydration process occurs. Several exothermic peaks on the DTA curve from ∼150 to ∼300 °C confirm the existence of the decomposition

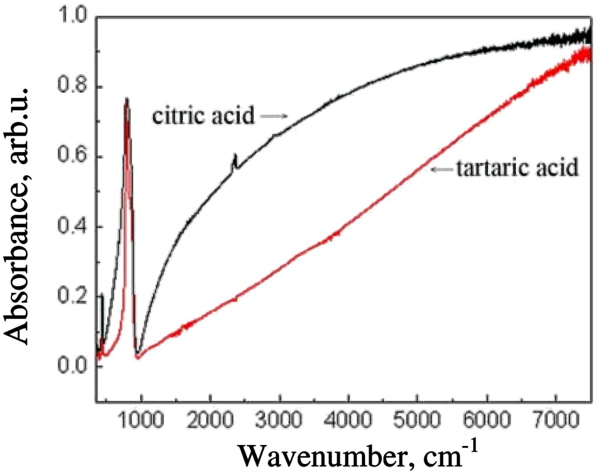

Fig. 3. Fragments from IR spectra of $CaWO_4$ samples sintered at 800 °C using two different complexing agents in the sol–gel processing.

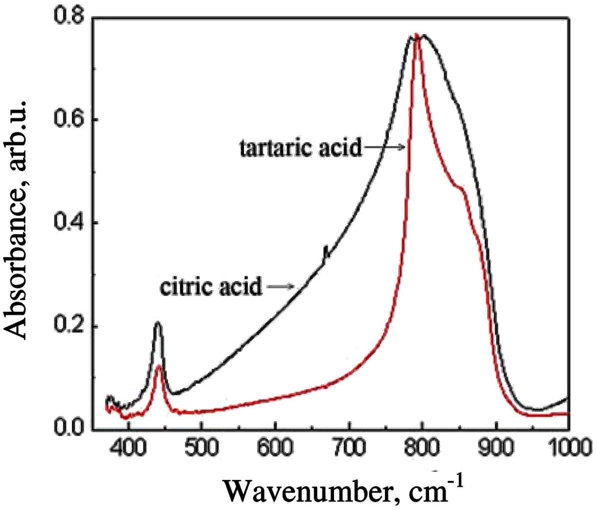

Fig. 4. Fragments from IR spectra of $CaWO_4$ samples sintered at 800 °C using two different complexing agents in the sol–gel processing.

processes during the heating of the precursor gel. Weak exothermic peaks at around 700 °C were also detected in the DTA curves of both gel samples. Interestingly, these exothermic peaks are not accompanied by weight loss on the TGA curves. Therefore, these endotherms probably correspond to the polymorphic transition of calcium tungstate.

Thus, the thermal characterization of the gel samples yields information about the mechanisms of thermal decomposition of the Ca-W-O gel precursor, and the optimum conditions for the final annealing can also be determined. According to the TG / DTA analysis data, the final annealing temperature for the preparation of $CaWO_4$ could be around 800 °C.

The Ca-W-O nitrate-tartrate and nitrate-citrate pre-

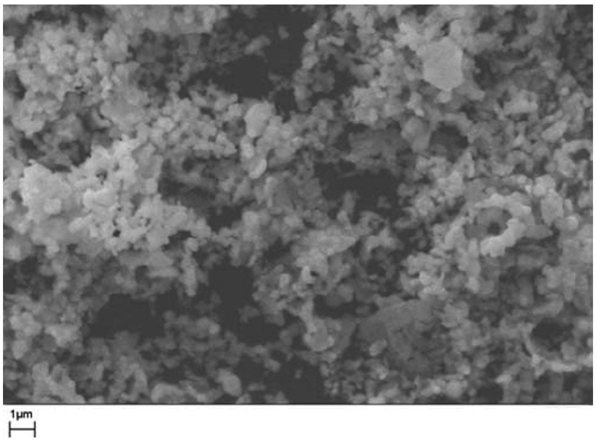

Fig. 5. SEM micrograph of $CaWO_4$ sample synthesized by TAS route. Magnification 20 k×.

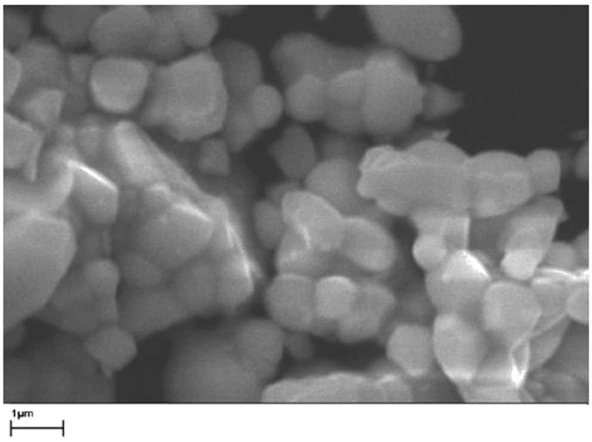

Fig. 6. SEM micrograph of $CaWO_4$ sample synthesized by CAS route. Magnification 20 k×.

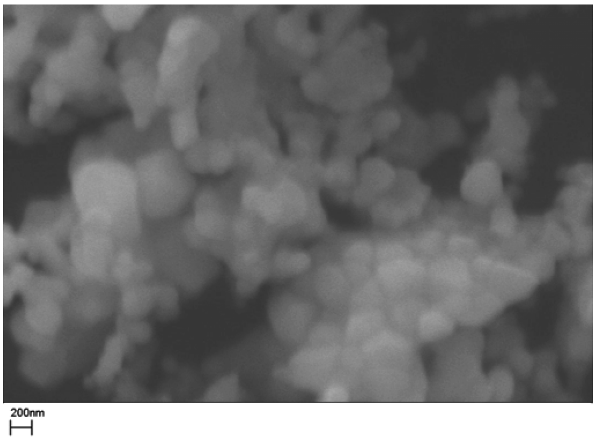

Fig. 7. SEM micrograph of $CaWO_4$ sample synthesized by TAS route. Magnification 65 k×.

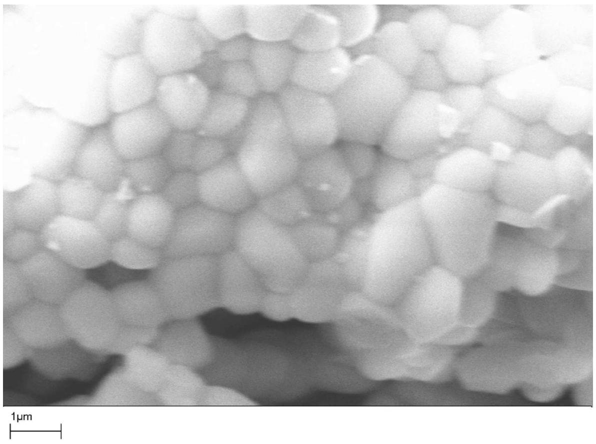

Fig. 8. SEM micrograph of $CaWO_4$ sample synthesized by CAS route. Magnification ×40k.

cursor gels were annealed at 800 °C to obtain $CaWO_4$ phase. The ceramic samples obtained were characterized by XRD analysis. The XRD patterns of $CaWO_4$ samples obtained by both TAS and CAS sol–gel routes were qualitatively the same regardless of the nature of the complexing reagent used in the sol–gel processing. The XRD patterns of synthesis products obtained by TAS and CAS sol–gel routes at 800 °C are compared in Fig. 2. As seen, the calcination of Ca-W-O nitrate-tartrate and nitrate-citrate precursor gels at 800 °C produces fully crystalline $CaWO_4$ phase. The most intensive lines are: (112), 100% (at $2\Theta \approx 28.5°$); (101), $\sim$48–51% (at around $2\Theta \approx 18.0°$); (204), $\sim$29–30% (at around $2\Theta \approx 47.3°$). This observation is in good agreement with previously reported results obtained for $CaWO_4$ phase [12]. Thus, the XRD data confirm that using tartaric or citric acids as complexing agents in the sol–gel process the single phase polycrystalline calcium tungstate was synthesized at 800 °C. The results let us to conclude that the proposed sol–gel synthesis routes could be very suitable methods to prepare the $CaWO_4$ phase homogeneously doped with lanthanide metal ions.

IR results were also found to be consistent with the crystallization process observed by XRD measurements. The fragments from IR spectra of $CaWO_4$ samples synthesized by two sol–gel routes are shown in Figs. 3 and 4. The IR spectra of the $CaWO_4$ samples calcined at 800 °C contain broad and intensive bands at 850–750 cm^{-1} which can be assigned to the characteristic vibrations of $WO_4{}^{2-}$ in scheelite [13, 14]. In addition, there are weaker bands at $\sim$445 cm^{-1}, which probably could be assigned to the characteristic metal–oxygen (Ca–O) vibrations [15]. Moreover, the IR spectra of calcium tungstate samples calcined at 800 °C do not show any bands attributable to carbonates or adsorbed water. The line broadening due to the local distortion of $WO_4{}^{2-}$ group in powders is also visible [9].

The textural properties of $CaWO_4$ powders obtained at 800 °C were investigated by SEM. The typical morphological photographs of $CaWO_4$ samples synthesized by TAS and CAS sol–gel routes are shown in Figs. 5 and 6, respectively. The SEM image of TAS derived $CaWO_4$ sample exhibits clustered grains made up of several tiny crystallites with a defined structure. It can be seen from Fig. 5 that the $CaWO_4$ solids are composed of plate-like and spherical grains. Individual particles seem to be nearly nano-sized crystals with an average particle size less than 1 μm. The SEM image of the $CaWO_4$ sample synthesized using citric acid in the sol–gel process (Fig. 6) also shows formation of crystallites less than 1 μm in size. However, it is evident that the CAS route produced slightly larger particles. Moreover, in the latter case the particles are formed with very well pronounced agglomeration, indicating a good connectivity between the grains. Evidently, the SEM results show that the morphological features of calcium tungstate are slightly dependent on the nature of the complexing agent used in the sol–gel processing. To estimate the grain size of synthesized calcium tungstate samples the SEM images at higher magnifications were recorded. The representative scanning electron micrographs of different $CaWO_4$ samples are shown in Figs. 7 and 8. The SEM images obtained at higher magnifications revealed highly agglomerated grains as well. Evidently, both sol–gel synthesis routes produce nanoparticles which have different mutual orientation. The SEM photograph of $CaWO_4$ ceramics synthesized using tartaric acid as a complexing agent in the sol–gel process shows dispersed nanocrystallites of nearly uniform size (∼350 nm). As already mentioned, the CAS derived $CaWO_4$ nanoparticles are slightly larger with the average grain size of ∼850 nm.

The luminescent properties of the $CaWO_4$ ceramics synthesized using sol–gel techniques were also investigated. Luminescence spectra under the pulse electron beam excitation of both $CaWO_4$ samples are shown in Figs. 9 and 10. Both spectra show a broad emission peak, which is very similar to that previously observed [16]. Moreover, the crystal size of $CaWO_4$ does not considerably affect the intensity of emission. In our case, the emission of CAS-derived $CaWO_4$ is just a little stronger than that obtained by the TAS route. Thus, we can conclude that larger particles produce slightly stronger luminescence.

4. Conclusions

Nanocrystalline $CaWO_4$ has been successfully synthesized by the simple sol–gel method using tungsten (VI) oxide and calcium nitrate tetrahydrate as starting materials. The complexing agents (citric and tartaric acids) used in the sol–gel processing have influence on the grain size and morphology of the final product. Photoluminescence (PL) measurements showed a broad emission peak in the blue region. Generally, in the proposed sol–gel synthesis route, the starting materials are of low cost and the synthesis processes are very simple, which should be a good choice as compared to the solid state method to synthesize $CaWO_4$ ceramics. This method can also be used to synthesize homogeneously doped $CaWO_4$ and related ceramics.

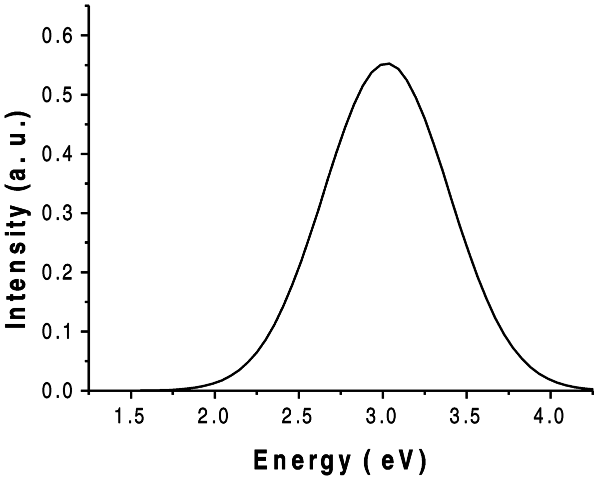

Fig. 9. Luminescence spectrum of $CaWO_4$ sample synthesized by TAS route.

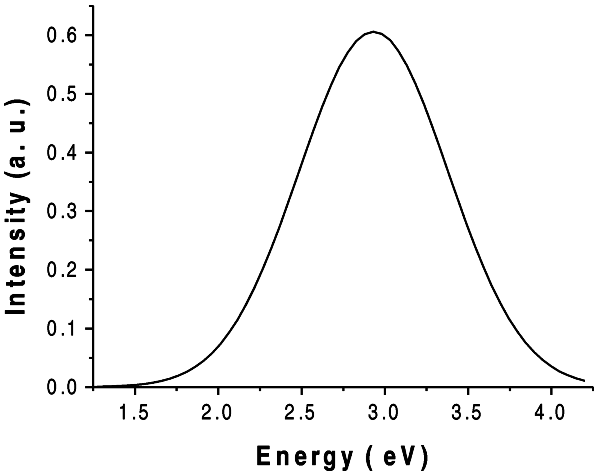

Fig. 10. Luminescence spectrum of $CaWO_4$ sample synthesized by CAS route.

Acknowledgements

The authors gratefully acknowledge Linas Vilčiauskas (Ulm University, Germany) for helpful discussions.

References

[1] R. Manalert and M.N. Rahaman, Sol–gel processing and sintering of yttrium aluminum garnet (YAG) powders, J. Mater. Sci. **31**, 3453–3458 (1996).

[2] E. Comini, A. Toncelli, M. Tonelli, E. Zannoni, E. Cavalli, A. Speghini, and M. Bettinelli, Optical spectroscopy and fluorescence dynamics of Er^{3+} in $Ca_3Sc_2Ge_3O_{12}$ crystal, J. Opt. Soc. Am. B **14**, 1938–1944 (1997).

[3] J.T. Vega-Duran, O. Barbosa-Garcia, L.A. Diaz-Torres, M.A. Meneses-Nava, and D.S. Sumida, Effects of energy back transfer on the luminescence of Yb and Er ions in YAG, Appl. Phys. Lett. **76**, 2032–2034 (2000).

[4] N.V. Kuleshov, A.A. Lagatsky, A.V. Podlipensky, V.P. Mikhailov, and G. Huber, Pulsed laser operation of Yb-doped $KY(WO_4)_2$ and $KGd(WO_4)_2$, Opt. Lett. **22**, 1317–1319 (1997).

[5] Y. Urata, T. Fukuda, H. Ito, and S. Wada, Laser performance of neodymium-doped lanthanum tungstate crystals, Jpn. J. Appl. Phys. **40**, 6453–6454 (2001).

[6] Y. Chen, X. Lin, Z. Luo, and Y. Huang, Spectroscopic properties of Nd^{3+} ions in $La_2(WO_4)_3$ crystal, Chem. Phys. Lett. **381**, 598–604 (2003).

[7] V.N. Kolobanov, I.A. Kamenskikh, V.V. Mikhailin, I.N. Shpinkov, D.A. Spassky, B.I. Zadneprovsky, L.I. Potkin, and G. Zimmerer, Optical and luminescent properties of anisotropic tungstate crystals, Nucl. Instrum. Methods A **486**, 496–503 (2002).

[8] V. Nagirnyi, E. Feldbach, L. Jonsson, M. Kirm, A. Lushchik, C. Lushchik, L.L. Nagornaya, V.D. Ryzhikov, F. Savikhiu, G. Svensson, and I.A. Tupitsina, Excitonic and recombination processes in $CaWO_4$ and $CdWO_4$ scintillators under synchrotron irradiation, Radiat. Meas. **29**, 247–250 (1998).

[9] P. Mogilevsky, T.A. Parthasarathy, and M.D. Petry, Anisotropy in room temperature microhardness and fracture of $CaWO_4$ scheelite, Acta Materialia **52**, 5529–5537 (2004).

[10] D.J. Norris, D.E. Arlinghaus, L. Meng, R. Heiny, and L.E. Scriven, Opaline photonic crystals: How does self-assembly work? Adv. Mater. **16**, 1393–1399 (2004).

[11] M. Remskar, Inorganic nanotubes, Adv. Mater. **16**, 1497–1504 (2004).

[12] S.J. Chen, J. Li, X.T. Chen, J.M. Hong, Z. Xue, and X.Z. You, Solvothermal synthesis and characterization of crystalline $CaWO_4$ nanoparticles, J. Cryst. Growth **253**, 361–365 (2003).

[13] L.J. Burcham and I.E. Wachs, Vibrational analysis of the two non-equivalent, tetrahedral tungstate (WO_4) units in $Ce_2(WO_4)_3$ and $La_2(WO_4)_3$, Spectrochim. Acta A **54**, 1355–1368 (1998).

[14] R.R. Khanna and E.R. Lippincott, Infrared spectra of some scheelite structures, Spectrochim. Acta A **24**, 905–908 (1968).

[15] E. Garskaite, K. Gibson, A. Leleckaite, J. Glaser, D. Niznansky, A. Kareiva, and H.-J. Meyer, On the synthesis and characterization of iron-containing garnets ($Y_3Fe_5O_{12}$, YIG and $Fe_3Al_5O_{12}$, IAG), Chem. Phys. **323**, 204–210 (2006).

[16] D. Chen, G. Shen, K. Tang, H. Zheng, and Y. Qian, Low-temperature synthesis of metal tungstates nanocrystallites in ethylene glycol, Mater. Res. Bull. **38**, 1783–1789 (2003).

NANOKRISTALINIO $CaWO_4$ SINTEZĖ ZOLIŲ IR GELIŲ METODU

A. Katelnikovas [a], L. Grigorjeva [b], D. Millers [b], V. Pankratov [b], A. Kareiva [a]

[a] *Vilniaus universitetas, Vilnius, Lietuva*

[b] *Latvijos universiteto Kietojo kūno fizikos institutas, Ryga, Latvija*

Santrauka

Zolių ir gelių metodu susintetintas nanokristalinis kalcio volframatas ($CaWO_4$) (pradinėmis medžiagomis buvo WO_3 ir $Ca(NO_3)_2 \cdot 4H_2O$). Citrinos ir vyno rūgštys buvo naudojamos kaip kompleksonai. Nustatyta, kad galutinio produkto morfologija ir gautų dalelių dydis priklauso nuo imtos rūgšties. $CaWO_4$ dalelių dydis svyravo nuo 350 iki 850 nm. Rezultatai parodė, kad iškaitinus gelius 800 °C temperatūroje susiformavo šelito kristalinės struktūros vienfazis $CaWO_4$, skleidžiantis mėlynos spektro srities šviesą. Susintetintas kalcio volframatas tirtas naudojant termogravimetrinės-diferencinės terminės analizės (TG / DTA), infraraudonosios spektrometrijos (IR), Rentgeno spindulių difrakcijos (XRD), skenuojančiosios elektroninės mikroskopijos (SEM) bei fotoliuminescencinės analizės (PL) metodus.